Journal of Thermal Analysis, Vol. 37 (1991) 1329-1346

Dedicated to Professor Dr. H. J. Seifert on the occasion of his 60th birthday

THE EFFECT OF STOICHIOMETRY ON THE IGNITION BEHAVIOUR OF SYNTHETIC PYRRHOTITES

J. G. Dunn and A. C. Chamberlain

SCHOOL OF APPLIED CHEMISTRY CURTIN UNIVERSITY OF TECHNOLOGY PERTH, WESTERN AUSTRALIA

(Received December 19, 1990)

A series of pyrrhotites of various stoichiometries was synthesized and characterized, and fractionated into four particle size ranges. The ignition temperatures and extent of reaction were determined by a thermogravimetric method. These measurements enabled the effect of stoichiometry and particle size on the ignition temperature and extent of oxidation to be established. The trends observed in the ignition behaviour are consistent with the concept of sulfur evolution being the key to the initiation of the ignition reaction.

The oxidation of sulfides in flash smelters proceeds by an ignition mechanism. By presenting the sulfide feed to a preheated furnace, the particles experience a heating rate of the order of thousands of degrees celsius per minute. At these rapid heating rates, the chemical energy produced by oxidation of the sulfide heats the particle rather than the environment. The particle temperature rises rapidly and an accelerating reaction proceeds which is self-driven and independent of the external conditions. This is typical of an ignition reaction, which is characterized by a single high energy emission which occurs in a very short time [1]. Factors affecting the ignition of sulfide materials are air temperature, oxygen concentration, furnace residence time, particle size and mineralogical composition [1–4].

Two important parameters in the study of ignition reactions are the:

(i) ignition temperature, which is defined as the minimum temperature required to provide a sufficient heating gradient to initiate an ignition reaction. Jorgensen [2] has pointed out that this value is not a thermodynamic constant and will vary with experimental conditions.

John Wiley & Sons, Limited, Chichester
Akadémiai Kiadó, Budapest

(ii) total extent of reaction (oxidation) of the mineral sulfide at various temperatures.

Several authors have proposed that ignition reactions in metals or coals are the result of interaction between a gaseous oxidant and a gaseous reductant [5-7]. With coal, for example, experimental results have indicated that the ignition is related to the temperature at which the rate of volatile loss becomes appreciable [8, 9].

Early reports on the ignition of sulfides suggested that oxygen diffusion into the sulfide particle was the controlling factor [10]. However, mathematical modelling has shown the diffusion of oxidant through a porous oxide layer is far too slow to account for the rapid reaction. Reaction times of 29 s have been calculated for oxidation of a zinc sulphide particle using the shrinking core model [5], in contrast to measured reaction times of less than 0.05 s for the ignition of sulfides [2].

More recently there have been suggestions that the ignition of sulfides occurs by gas phase redox reactions, analogous to those of the metals and coal. This involves either the evolution of sulfur vapour by pyrolytic decomposition of the parent sulfide, such as occurs in chalcopyrite [11], or the evolution of metal sulfide molecules as in the cases of zinc [5] or lead [12].

The literature to date has reported the ignition behaviour of specific naturally-occuring mineral sulfides. No publications are evident on a systematic study of the effect of stoichiometry, in particular the metal: sulfur ratio, on the ignition behaviour.

Experimental

Preparation of synthetic pyrrhotites $Fe_{(1-x)}S$

Pyrrhotites of various stoichiometries were made by mixing together iron and sulfur (99.95% purity, Aldrich Chemical Company) in sealed evacuated silica tubes and heating at 780° for 24 h. The silica tubes were removed from the furnace and rapidly quenched in water.

Each synthetic pyrrhotite was sieved through Brass Endecott Laboratory Test Sieves to isolate the 125–90, 90–63, 63–45 and $<45\,\mu$m fractions. Fines were removed from the $<45\,\mu$m fraction by suspending the material in distilled pentane using an ultrasonic bath and filtering through a 20 μm nylon sieve to produce a 45–20 μm fraction.

Characterization of synthetic pyrrhotites

Iron and sulfur were determined by wet chemical analysis.

A Cameca SX50 Electronprobe Microanalyser (EPMA) interfaced with a digital PDP11 mainframe computer was employed to determine the iron and sulfur contents of at least 20 particles. For several particles iron and sulfur were determined at five spots across the particle. All results were processed using a simple ratio between the detector counts per second per nanoamp (nA) for standard and unknown material.

X-ray diffraction (XRD) patterns were acquired using a Siemens D500 Diffractometer with Cu K_α ($\lambda = 1.5418$ Å) radiation and graphite monochromator. X-ray spectra were analysed on Socabim data analysis software in conjunction with JCPDS–X-ray spectra search and match analysis.

Scanning electron microscopy (SEM) was performed on samples embedded in epoxy resin using a JEOL JSM–35C instrument fitted with an X-ray energy dispersive spectrometer (EDS–Si(Li) detector). Secondary and backscattered electron images were collected using an accelerating voltage of 25 keV. X-ray energy spectra were obtained using a TN–1075 multichannel analyser interfaced with an IBM compatible computer. E_K characteristic X-rays were identified and plotted on a X–Y plotter. Micrographs were taken using a 120 format camera.

Surface-area measurement were determined by the Brunauer, Emmett and Teller (BET) method.

Thermal analysis

Ignition temperatures were measured using a Stanton Redcroft TG–750 thermobalance. 5 mg samples were weighed into platinum sample crucibles, 5 mm in diameter and 2 mm in depth. An oxygen atmosphere was established in the furnace at a flowrate of 25 $ml \cdot min^{-1}$. The furnace was situated directly below the sample crucible. An asbestos plate was positioned over the furnace while a sample was being weighed into the sample crucible. The furnace was preheated to a set temperature between 500° and 900°, and then raised around the sample. If no significant reaction occurred, the furnace was lowered, the temperature increased by 5°, and raised around a fresh sample. This process was repeated until the sample ignited, as indicated by a rapid mass loss. The measurements were repeated in triplicate.

The extent of reaction at any particular furnace temperature is directly proportional to the observed mass loss at that temperature. The maximum

mass loss occurred at 900°. The extent of reaction was calculated at the ignition temperature.

$$\text{Percentage extent of reaction} = \frac{(\text{mass loss at } T^\circ \cdot 100)}{(\text{mass loss at } 900^\circ\text{C})}$$

Partially oxidized samples were produced by heating samples under non-ignition conditions in the apparatus at 20 deg·min^{-1} in an air atmosphere, stopping the heating programme at a predetermined point and changing the atmosphere to nitrogen. The products were examined by XRD and SEM.

Results and discussion

Characterization of samples

The analytical results obtained by wet chemical methods and EPMA are presented in Tables 1 and 2 respectively.

Table 1 Iron and sulfur content of pyrrhotites determined by wet chemical analysis

Synthetic pyrrhotite	Composition			
	% Fe	% S	TOT %	Fe(1–x)S
1	59.0	40.3	99.3	Fe0.83S
2	60.6	36.8	97.4	Fe0.88S
3	61.7	38.7	100.4	Fe0.92S
4	62.7	38.5	101.5	Fe0.96S
5	63.6	35.6	99.2	Fe1.00S

Table 2 Iron and sulfur ratios in pyrrhotites determined by EPMA

Synthetic pyrrhotite	Composition			
	Atomic mass ratio		Stoichiometry	Error
	Av. Fe	Av. S	Fe(1–x)S	(1–x)
1	0.4584	0.5416	Fe0.85S	0.01
2	0.4692	0.5308	Fe0.88S	0.003
3	0.4802	0.5198	Fe0.92S	0.005
4	0.4903	0.5097	Fe0.96S	0.004
5	0.4967	0.5033	Fe0.99S	0.01

Although the results differ slightly between the two methods, the calculated stoichiometries are within experimental error. Since the EPMA results were obtained on a minor fraction of the total sample population, the composition of each synthetic pyrrhotite was taken to be that obtained from the wet chemical analysis.

Results from a five point analysis across several particles of $Fe_{0.83}S$ are presented in Table 3. Pyrrhotite was the only phase detected. Similar results were obtained for $Fe_{0.88}S$ and $Fe_{0.92}S$. Although the iron to sulfur ratio varied slightly within each particle, the mean stoichiometry from the individual transverse scans agreed well with the wet chemical and EPMA results shown in Tables 1 and 2 respectively. From these results it can be concluded that the pyrrhotite particles within each sample are homogeneous.

Table 3 Composition of $Fe_{0.83}S$ determined by EPMA at five different points on five particles

Particle	Number of scans				
	1	2	3	4	5
1	Fe0.850S	Fe0.850S	Fe0.857S	Fe0.853S	Fe0.849S
2	Fe0.838S	Fe0.845S	Fe0.851S	Fe0.848S	Fe0.853S
3	Fe0.853S	Fe0.853S	Fe0.854S	Fe0.848S	Fe0.847S
4	Fe0.829S	Fe0.845S	Fe0.840S	Fe0.839S	Fe0.840S
5	Fe0.838S	Fe0.842S	Fe0.838S	Fe0.839S	Fe0.840S

The XRD patterns of the samples identified pyrrhotite as the only phase present. The recorded 2–theta angle of reflectance for the d_{102} lattice spacing systematically decreased as the stoichiometry changed from $Fe_{0.83}S$ to FeS, a trend previously noted by others [13, 14].

SEM of the particles showed that the surfaces were generally smooth with a metallic lustre. As the stoichiometry of the pyrrhotites decreased, the number of holes and imperfections increased. However, surface area measurements made on $Fe_{0.92}S$ and FeS showed little variation in the surface area with change in stoichiometry, with values of 0.124 and 0.133 $m^2 \cdot g^{-1}$ respectively. Such low values indicate that the synthetic pyrhotites are extremely non-porous.

Pyrolysis reactions

The synthetic pyrrhotites were heated in the TG apparatus in a nitrogen atmosphere. The TG curves are presented in Figs 1 and 2 for particle sizes

45–63 and 90–125 μm respectively. All except $Fe_{0.83}S$ showed similar behaviour, with no appreciable change until the decomposition temperature of the sulfide was reached. Then a gradual mass loss was evident which can be attributed to the evolution of sulfur. The decomposition temperatures are given in Table 4. It is evident that the decomposition temperature decreases as the sulfide becomes increasingly iron deficient, with the exception of the FeS/$Fe_{0.96}S$ pair in the 45–63 μm particle size, in which the order is reversed. A change in particle size has relatively little effect on decomposition temperature. The amount of sulfur liberated increased at any specific temperature as the compounds became less stoichiometric.

Table 4 Decomposition temperatures of the 90–125 μm and 45–63 μm fractions for the pyrrhotites determined by TG

Synthetic pyrrhotite	Decomposition temperatures, °C	
	90–125 μm	45–63 μm
Fe0.83S	500	515
Fe0.88S	575	580
Fe0.92S	650	620
Fe0.96S	625	635
Fe1.00S	680	670

The $Fe_{0.83}S$ exhibited a two-stage mass loss, the first one being a discrete mass loss at 550–600°. Based on the first mass loss, the reaction can be represented by;

$$Fe_{0.83}S \rightarrow Fe_{0.86}S + 0.03S$$

The product then decomposed on further heating in the same manner as the other pyrrhotites. The combined two stage mass loss corresponded to significantly more sulfur than evolved from the other pyrrhotites.

Ignition temperature measurements

The ignition temperature and total extent of reaction were determined for each synthetic pyrrhotite sample using the isothermal TG method described in the experimental section. The average time lapsed between the introduction of the 5 mg sample into the pre-heated furnace and the commencement of the ignition reaction was approximately 7 s. This equates to a heating rate of approximately 5000 deg·min^{-1}.

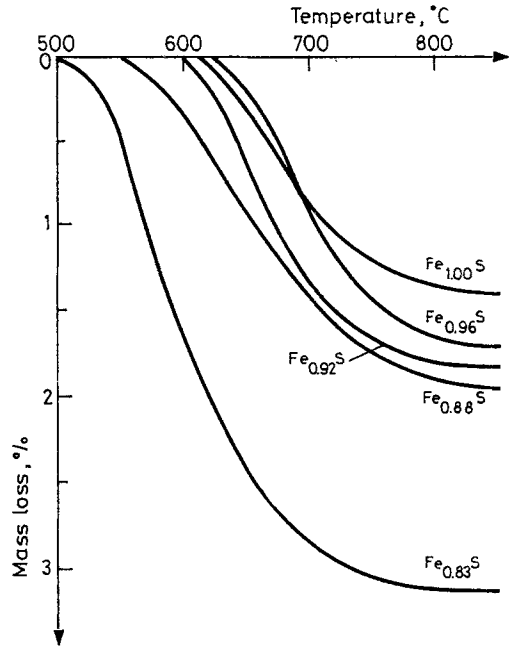

Fig. 1 TG curves for the decomposition of the pyrrhotites in nitrogen. 45–63 μm

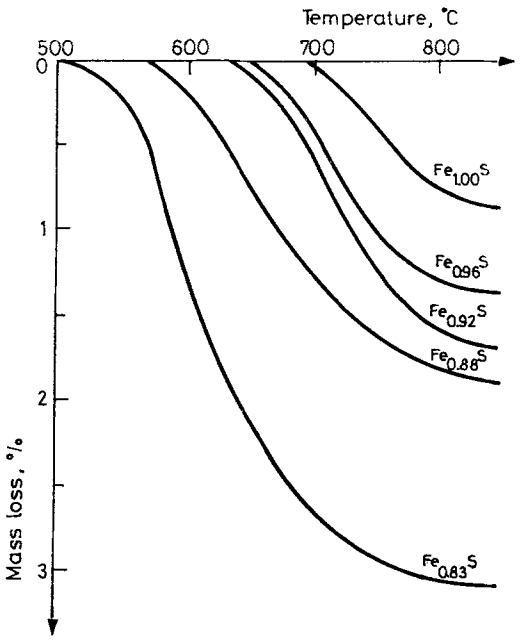

Fig. 2 TG curves for the decomposition of the pyrrhotites in nitrogen. 90–125 μm

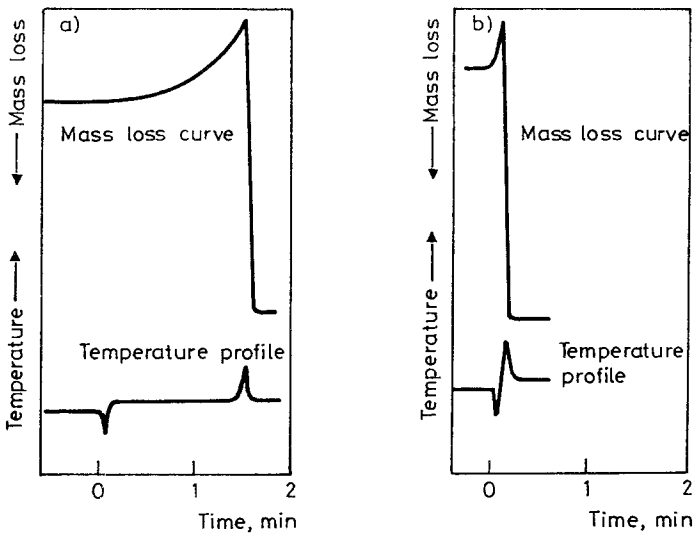

Fig. 3 Typical TG curves from the isothermal technique used to measure the ignition temperatures of the pyrrhotites. (a) Non-ignition, (b) Ignition

Below the ignition temperature there was a slow mass gain due to the formation of sulfate, as illustrated in Fig. 3a. This was immediately followed by a mass loss due to oxidation of unreacted pyrrhotite. This process typically occurred over a 1–2 min period.

The difference in furnace temperature required to convert from non-ignition to ignition was only 5°. A typical TG curve for a sample at the ignition temperature is shown in Fig. 3b. During the induction period a mass gain is observed, which can be assigned to the formation of sulfate. This is followed by a rapid mass loss of 8–13% corresponding to the oxidation of the sulfide material. The sample had undergone complete oxidation after approximately 20 s. The final product was hematite confirmed by XRD and EDS. The overall reaction is given by the following equation:

$$4Fe_{(1-x)}S + (7-3x)O_2 \rightarrow (2-2x)Fe_2O_3 + 4SO_2$$

The sample shows a large temperature excursion from the linear temperature profile due to the energy evolved from the rapid oxidation of the sulfide material. The temperature excursion increases in intensity as the pyrrhotite stoichiometry decreases, that is as the sulfur excess increases.

The measured ignition temperatures are presented in Table 5. Figure 4 illustrates the effect of stoichiometry on the ignition temperature. A sig-

nificant decrease in ignition temperature occurred as the composition of the pyrrhotites changed from FeS to $Fe_{0.83}S$. If the coarsest fraction of particle size 90–125 μm is considered, FeS showed an ignition temperature of 755° compared to a value of 545° for $Fe_{0.83}S$, a difference of 210°. This was not a smooth trend, however, as the difference between FeS and $Fe_{0.88}S$, with ignition temperatures of 755 and 660° respectively, was only 95°. Hence a change in stoichiometry of 0.12 produces a difference in ignition temperature of 95°, whilst a change of 0.05 (the difference between $Fe_{0.88}S$ and $Fe_{0.83}S$) produces a disproportionate difference of 115°.

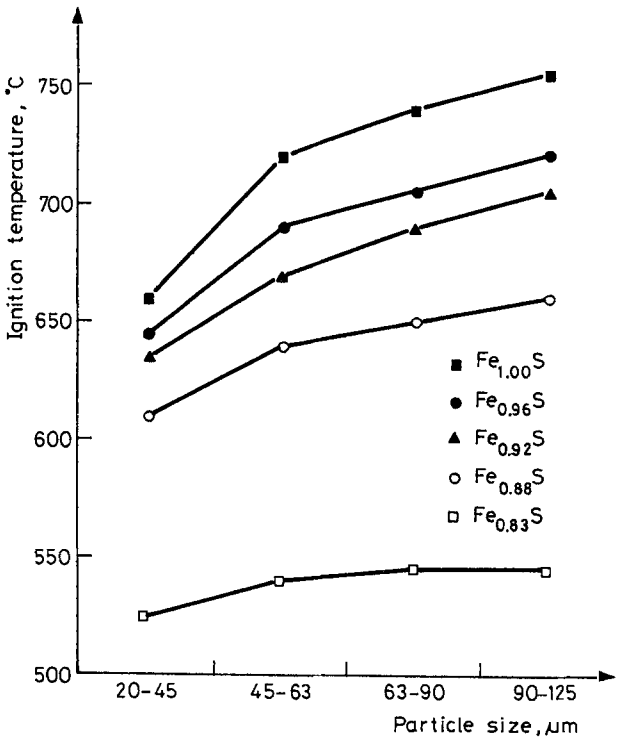

Fig. 4 Effect of stoichiometry and particle size of pyrrhotites on their ignition temperatures

A decrease in the ignition temperature was observed as the particle size decreased. The end column in Table 5 gives the difference in the ignition temperature between the 90–125 μm and 20–45 μm particle size fraction for each synthetic pyrrhotite. The effect was not constant, and decreases as the stoichiometry of the synthetic pyrrhotite decreases. The ignition temperature for FeS showed the largest decrease with particle size of 95°, compared

with only a 20° decrease from $Fe_{0.83}S$. This is evident in Fig. 4. As the particle size decreases the ignition temperature curves converge.

Table 5 Ignition temperatures of the pyrrhotites determined by the isothermal TG method

Synthetic pyrrhotite	Ignition temperature, °C				
	20–45 μm	45–63 μm	63–90 μm	90–125 μm	Change
Fe0.83S	525	540	545	545	20
Fe0.88S	610	640	650	660	50
Fe0.92S	635	670	690	705	70
Fe0.96S	645	690	705	720	75
Fe1.00S	660	720	740	755	95

At the ignition temperature all the pyrrhotite samples showed 95–100% extent of reaction (see Table 6), and this appeared to be independent of the particle size. It is reasonable to infer that the oxidation of pyrrhotite tends to go to completion once vigorous enough conditions to promote its ignition have been reached. In this respect the pyrrhotites differ from iron-nickel sulfides, where extent of oxidation is variable with temperature [1].

SEM examination of oxidized products

To obtain information on any change in reaction mechanism, samples of the unfractionated pyrrhotites were obtained from both non-ignition and ignition conditions and examined by SEM. Samples from non-ignition conditions were collected at the start of the first major mass loss, part way through the mass loss and at the end of the mass loss. No significant reaction had occurred for particles of FeS heated to 615° (Fig. 5a). Apart from a thin rim of reacted material, the particles had the same smooth metallic lustre as the starting substance. Further heating to 660° showed particles to have undergone a considerable extent of oxidation, which occurred along the basal spacing planes as shown in Fig. 5b. The particles had not reacted uniformly, and some parts of the particles presented as unreacted whilst other parts were well oxidized. At 750° the particles had completely oxidized (Fig. 5c). A similar set of micrographs was obtained for $Fe_{0.83}S$. The oxidation reactions commenced and finished at lower temperatures relative to FeS. No reaction was apparent until 500° (Fig. 5d), but significant oxidation had occurred by 595° (Fig. 5e). The reaction was complete at 700° (Fig. 5f).

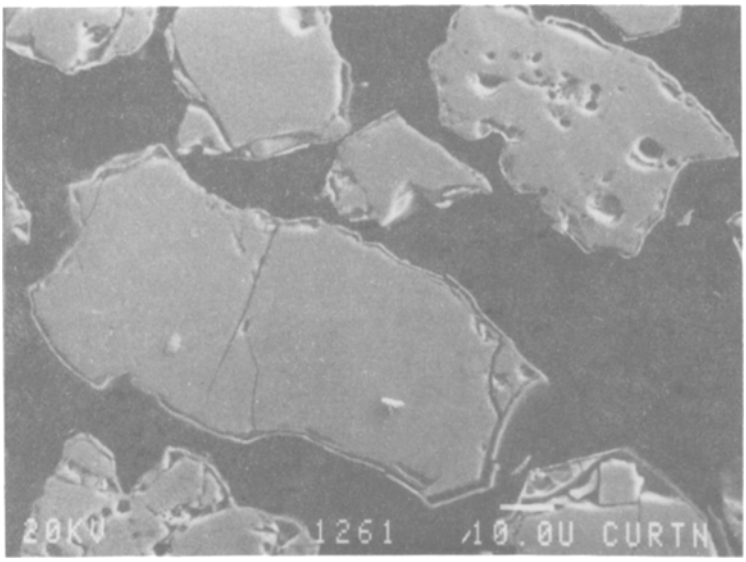

Fig. 5a SEM micrograph of oxidized pyrrhotites FeS heated to 615°

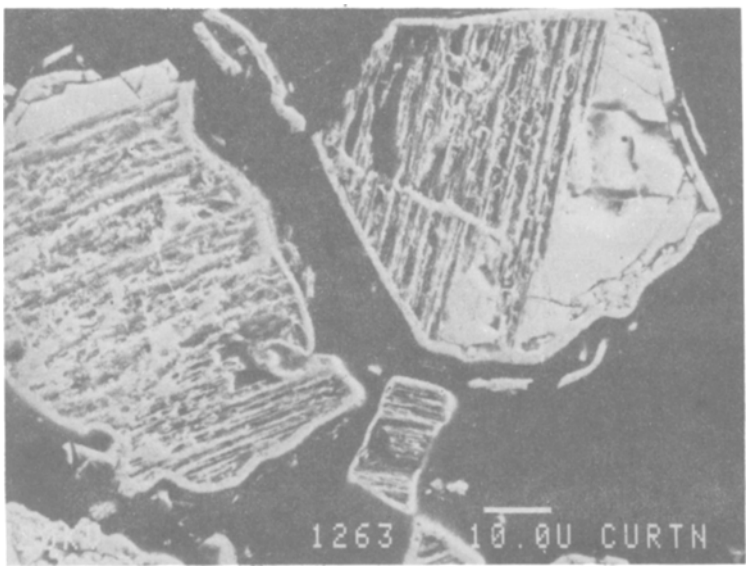

Fig. 5b SEM micrographs of oxidized pyrrhotites FeS heated to 660°

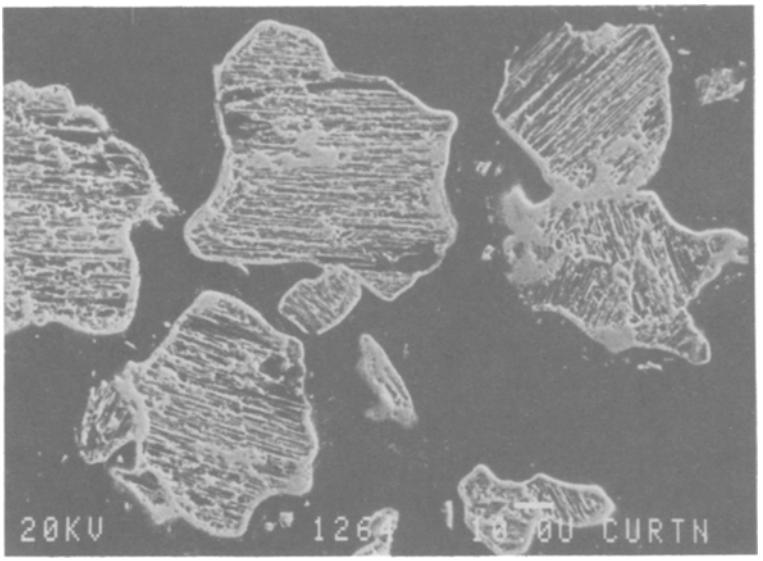

Fig. 5c SEM micrograph of oxidized pyrrhotites FeS heated to 750°

Figures 5g and 5h show two micrographs of FeS and $Fe_{0.83}S$ respectively which have undergone ignition. The particle morphology was quite different to that shown by the non-ignited samples. No oxidation along the basal spacings was evident. The structure was completely random and quite porous, suggesting that rapid gas evolution had occurred.

Table 6 Extent of oxidation for the pyrrhotites

Synthetic pyrrhotite	Extent of reaction, %			
	20–45 μm	45–63 μm	63–90 μm	90–125 μm
Fe0.83S	100	100	100	100
Fe0.88S	99	100	96	100
Fe0.92S	100	100	100	100
Fe0.96S	100	100	95	98
Fe1.00S	100	100	96	96

Ignition mechanism

An important subsidiary aim of this work was to consider the mechanism of the ignition reaction. The characterization procedures have indicated that the synthetic pyrrhotites consist of homogeneous compounds with no other

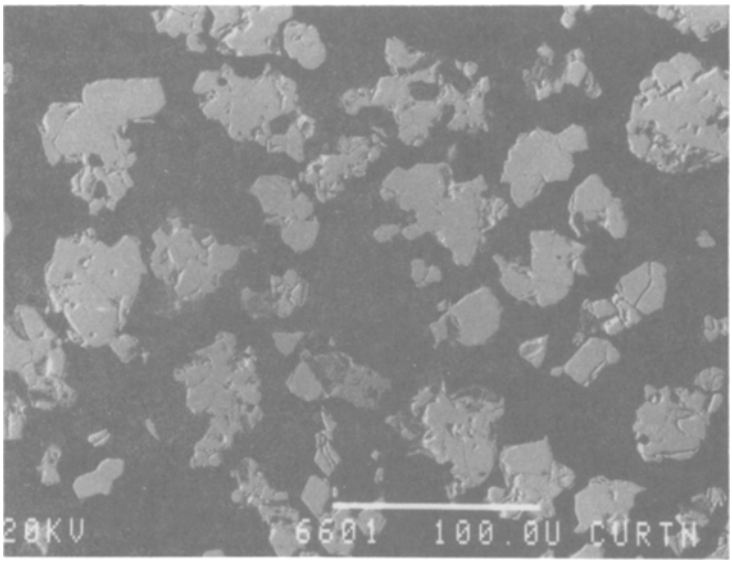

Fig. 5d SEM micrograph of oxidized pyrrhotites $Fe_{0.83}S$ heated to 500°

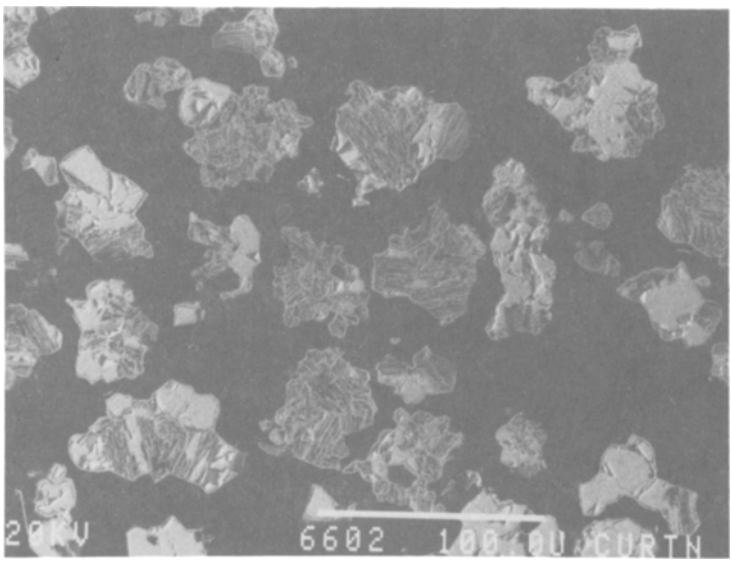

Fig. 5e SEM micrograph of oxidized pyrrhotites $Fe_{0.83}S$ heated to 595°

sulfidic species present. Their surface areas are similar, and fractions of similar particle size were available. Hence the only variable is the iron:sulfur ratio.

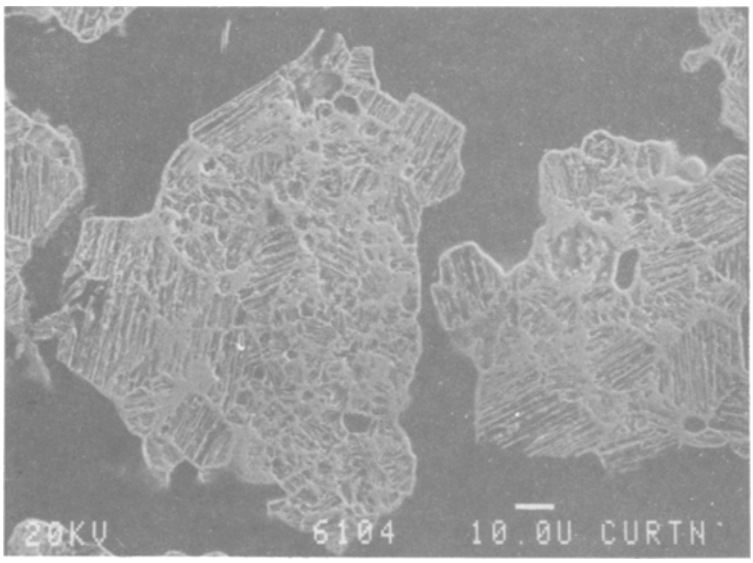

Fig. 5f SEM micrograph of oxidized pyrrhotites $Fe_{0.83}S$ heated to 700°

Figure 6 shows a plot of the decomposition temperature against the ignition temperature for the five synthetic pyrrhotites at two different particle sizes. This shows that the decomposition temperature decreases regularly with the ignition temperature. In all cases the decomposition temperature is lower than the ignition temperature, indicating that decomposition and release of sulfur occurs prior to ignition. The curves are approximately parallel, suggesting that the difference between decomposition and ignition temperatures was affected to the same extent by particle size.

The only irregular point in Fig. 6 is that for $Fe_{0.83}S$, and this is due to the disproportionate decrease in ignition temperature between this compound and the previous one (see Fig. 4). This can be explained by the relatively large and discrete quantity of sulfur released from $Fe_{0.83}S$ in the temperature range 550–600°. The burning of sulfur on the surface of the particle produces considerable heat energy, which would heat the particle to higher temperatures, causing more sulfur to vaporize and thus accelerating the rate of reaction. Clearly the more sulfur released, the greater will be the heating

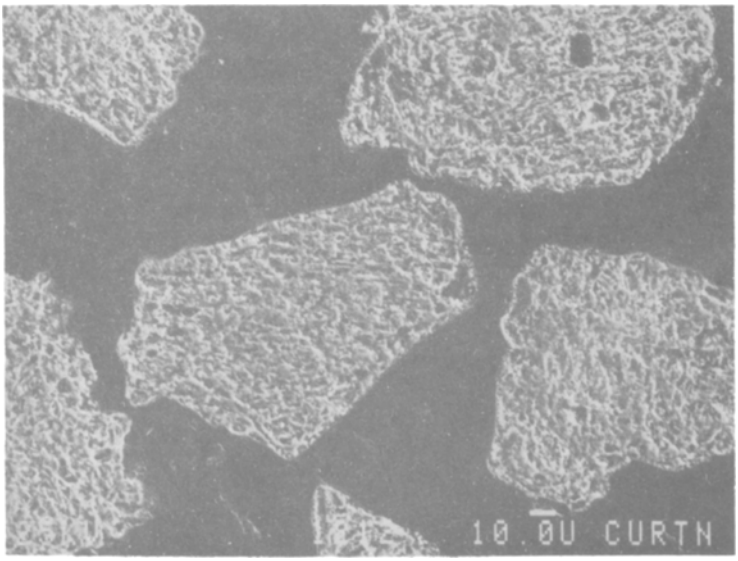

Fig. 5g SEM micrograph of oxidized pyrrhotites Ignited FeS

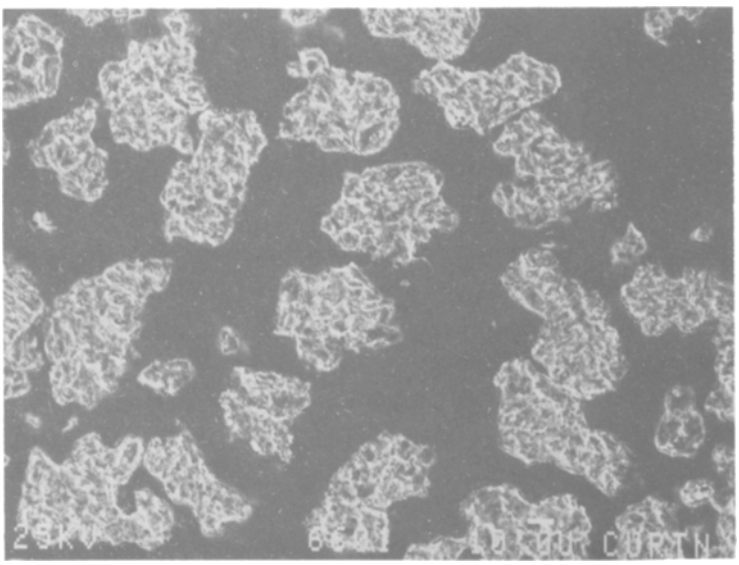

Fig. 5h SEM micrograph of oxidized pyrrhotites Ignited $Fe_{0.83}S$

effect, and the more likely the sulfide is to ignite. This argument is supported by the excursion from the set furnace temperature once ignition occurs, since the excursion increased as the pyrrhotites became more sulfur rich.

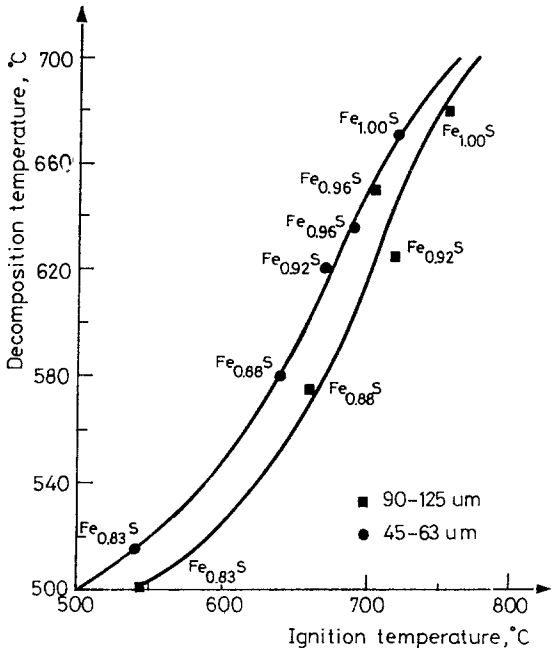

Fig 6 Plot of decomposition temperature against ignition temperature for the pyrrhotites for two different particle sizes

This process can also be used to explain the decreasing sensitivity to particle size effects as the compounds become more sulfur rich. Figures 1 and 2 show that at a specific temperature more sulfur is released as the pyrrhotites become more sulfur rich. The more sulfur that is released and subsequently oxidized, the greater will be the ease of ignition. If the quantity of heat released is more than enough to heat the particle and sustain the evolution of sulfur, then particle size will decrease in importance.

Conclusion

It has been demonstrated that a clear relationship exists between the stoichiometry of a series of pyrrhotites and their ignition temperature, with the latter decreasing as the pyrrhotite composition became increasingly sul-

fur rich. The effect is significant, with a decrease in ignition temperature of 210° between FeS and $Fe_{0.83}S$ for the coarsest fraction. Once ignited, the oxidation reaction proceeded to completion.

The ignition temperature showed a decrease with decreasing particle size. This effect was most evident for FeS, and decreased as the pyrrhotites became increasingly sulfur rich.

There is a significant relationship between the decomposition temperature of the pyrrhotites and their ignition temperatures, with a decrease in decomposition temperature producing a concomitant decrease in the ignition temperature.

The ignition behaviour of the pyrrhotites is consistent with the evolution of sulfur being the rate controlling factor.

The practical implication of this work is that to assess the ease of ignition and hence flash smelting of pyrrhotites requires information about their stoichiometry. If this finding is more generally applicable, then knowledge of the mineralogical composition of a flash smelter feedstock alone is not sufficient to assess the smelting behaviour, and the actual stoichiometry of the mineral is required.

* * *

We are grateful to Dr. B. Robinson of the CSIRO Division of Mineral Products, Perth, for making available the microprobe equipment and assisting in the collection of data.

References

1 J. G. Dunn, A. Jayaweera and S. G. Davies, Proc. Australas. Inst. Min. Metall., 290 (1985) 75.
2 F. R. A. Jorgenson, Proc. Australas. Inst. Min. Metall., 268 (1978) 47.
3 T. N. Smith, J. G. Dunn, L. C. Mackey and I. R. Stevenson, Report No. 39, (1988), Minerals and Energy Research Institute of Western Australia.
4 J. G. Dunn, S. G. Davies and L. C. Mackey, Proc. Australas. Inst. Min. Metall., 294 (1989) 57.
5 I. Barin, M. Modigell and F. Sauert, Thermodynamics and kinetics of cyclone smelting, in H. Y. Sohn, D. B. George and A. D. Zunkel (eds), Advances in Sulphide Smelting, Proc. International Sulphide Smelting Symposium, Metall. Soc. AIME, Vol 1, 1983 p. 257.
6 H. Juntgen, EPE, Rev. Energ. Primaire, 12 (1976) 11.
7 M. A. Nettleton and R. Stirling, Proc. Roy. Soc. Ser. A, 300 (1967) 62.
8 S. Yuasa and T. Takeno, Nineteenth Symposium (International) on Combustion, The Combustion Institute, (1982) 741.
9 L. S. Merril, Fuel, 52 (1973) 61.
10 N. J. Themelis and H. H. Kellogg, Principles of Sulphide Smelting, in H. Y. Sohn, D. B. George and A. D. Zunkel (eds), Advances in Sulfide Smelting, Proc. International Sulfide Smelting Symposium, Metall. Soc. AIME, Vol. 1, 1983 p. 1.
11 Y. H. Kim, Studies of the rate phenomena in particulate flash reaction systems: Oxidation of metal sulfides, PhD thesis, (1987) Columbia University.

12 F. R. A. Jorgenson, Australian Japan Extractive Metallurgy Symposium, Australas. Inst. Min. Metall., (1980) 41.
13 R. G. Arnold, Economic Geology, 57 (1962) 72.
14 P. Toulmin and P. B. Barton, Geochim. Cosmochim. Acta, 28 (1964) 641.

Zusammenfassung — Es wurde eine Reihe Pyrrhotine unterschiedlicher Zusammensetzung hergestellt, beschrieben und nach Partikelgröße in vier Fraktionen zerlegt. Zündungstemperatur und Reaktionsausmaß wurden thermogravimetrisch bestimmt. Durch diese Messungen wurde es ermöglicht, den Einfluß von Stöchiometrie und Partikelgröße auf Zündungstemperatur und Oxidationsausmaß zu schätzen. Die beim Zündungsverhalten beobachteten Tendenzen stimmen mit dem Konzept überein, wonach die Freisetzung von Schwefel zum Einsetzen der Zündungsreaktion führt.